REDVET - Revista electrónica de Veterinaria - ISSN 1695-7504
Vol 25, No. 1 (2024)
http://www.veterinaria.org
Article Received:25-02-2024 Revised: 10-03-2024 Accepted: 15-03-2024

Facile Biosynthesis of ZnO nanoparticles using Gracilaria textorii extract: Characterization and evaluation of photocatalytic and biological performance

J. Mukila[1], S. Sankaravadivu[1*], V.Priya[2]

[1]Research Scholar (Reg-No 23112012032001), [1,1*,2] PG & Research Department of Chemistry, A.P.C Mahalaxmi College for women, Thoothukudi, Affiliated to Manonmaniam sundaranar University, Abishekapatti, Tirunelveli-627012, Tamil Nadu, India.

Abstract:
Zinc oxide (ZnO) nanoparticles have physico-chemical methods, such as cost effectiveness; reduce toxicity, and environment sustainability. The present study green synthesis of ZnO nanoparticles using the red algae *Gracilaria textorii* as a natural reducing and stabilizing agent. The optical properties of the synthesized nanoparticles were confirmed by UV–Vis spectroscopy, which exhibited a characteristic absorption peak at 347 nm. FTIR analysis revealed the presence of Zn–O stretching vibrations within the range of 400–600 cm^{-1}, confirming the formation of ZnO. XRD analysis demonstrated the crystalline nature of the nanoparticles, with an average crystallite size of 34.8 nm. FESEM micrographs showed flake-like nanosheet morphology with particle agglomeration, while EDX analysis verified the elemental composition, consisting of 71.82% Zn and 28.18% O. Furthermore, DLS measurements indicated a polydispersity index of 0.351, suggesting a moderately uniform particle size distribution. Electrochemical studies performed using cyclic voltammetry revealed quasi-rectangular voltammograms with distinct anodic and cathodic responses, indicating efficient charge-transfer characteristics. The photocatalytic activity of the ZnO nanoparticles was assessed through the degradation of methylene blue dye under sunlight irradiation, achieving a degradation efficiency of 76% within 70 min. In addition, the synthesized nanoparticles exhibited considerable antioxidant activity in both DPPH and H_2O_2 radical scavenging assays. Significant antibacterial activity was also observed against *Escherichia coli, Staphylococcus aureus,* and *Pseudomonas aeruginosa*, demonstrating effectiveness against both Gram-positive and Gram-negative bacterial strains. Overall, the findings highlight the potential of biosynthesized ZnO nanoparticles as multifunctional materials for environmental remediation and biomedical applications.

Keywords: *Gracilaria textorii*, Methylene Blue, Red algae, Antibacterial, Antioxidant, Zinc Oxide

1. INTRODUCTION:

Nanotechnology is the science of manipulating matter at the nanoscale to create new and unique materials and products with enormous potential to change environment[1,2].zinc oxide nanoparticle has promoted itself as an interesting metal oxide material because of its unique physical and chemical properties such as high chemical and mechanical stability, broad range of radiation absorption, high catalytic activity,[3] good electrical conductivity, non toxic and environmentally friendly nature etc.,[4,5] Zinc oxide is a unique semiconducting material and lot of other interesting applications. its widely used as biosensor, solar cells, [6] chemical sensor, gas sensor, photo detectors, catalysts, active fillers for rubber [7,8] and plastics, optical material, additive in treatment of water and waste water etc.[9,10] However most ZnO nano-particles used commercially produced synthetically which have some advantages, compared to silver nano-particle, such as lower cost, white appearance [11]. The antibacterial agents are used to prevent or kill the growth of bacteria. Zinc oxide nanoparticles are excellent antibacterial drug activity compared to that of the bulk material [12]. Several studies have successfully been led to synthesize ZnO nanoparticles using different organisms such as bacteria, fungi, algae, and plants. [13] Algae are being used more and more in green synthesis because of their abundant secondary metabolites, quick growth rate, ease of harvesting, and affordable scale-up[14] Marine macroalgae are important ecologically and commercially to many regions of the world, especially in Asian countries such as China, Japan and Korea [15]. Seaweeds are classified into three main category: brown algae (phaeophyta), green algae (chlorophyta), and red algae (rhodophyta)[16]. Red algae are a widespread group of uni- to multicellular aquatic photoautotrophic plants. Planktonic unicellular species have simple life cycles characterized by regular binary cell division. [17] Red algae, or Rhodophyta, are one of the oldest groups of eukaryotic algae. The Rhodophyta comprises one of the largest phyla of algae, containing over 7,000 currently recognized species with taxonomic revisions ongoing. [18] Among marine organisms, marine algae are rich sources of structurally diverse bioactive compounds with various biological activities. Recently, their importance as a source of novel bioactive substances is growing rapidly and researchers have revealed that marine algal originated compounds exhibit various biological activities [19] The synthesized ZnO nanoparticles were comprehensively characterized using UV–Visible spectroscopy, X-ray diffraction (XRD), Fourier transform infrared (FTIR) spectroscopy, field emission scanning electron microscopy coupled with energy-dispersive X-ray spectroscopy (FESEM–EDX), and dynamic light scattering (DLS) analysis. The photocatalytic efficiency of the synthesized ZnO nanoparticles was subsequently investigated through the degradation of methylene blue (MB) dye under irradiation conditions. In addition, their antibacterial activity was evaluated against pathogenic bacterial strains, namely *Escherichia coli*, *Staphylococcus aureus*, and *Pseudomonas aeruginosa*. The antioxidant

REDVET - Revista electrónica de Veterinaria - ISSN 1695-7504
Vol 25, No. 1 (2024)
http://www.veterinaria.org
Article Received:25-02-2024 Revised: 10-03-2024 Accepted: 15-03-2024

potential of the nanoparticles was further assessed using DPPH and hydrogen peroxide (H_2O_2) radical scavenging assays. The findings highlight the multifunctional nature of the synthesized ZnO nanoparticles and demonstrate their potential for biological and environmental applications.

2. Materials and Methods:

Zinc nitrate hexahydrate [$Zn(NO_3)_2 \cdot 6H_2O$] and sodium hydroxide (NaOH) of analytical grade were used as precursor materials for nanoparticle synthesis. Double-distilled deionized (DI) water was employed throughout the experimental procedures, and filtration was carried out using Whatman No. 1 filter paper. A zinc nitrate solution was prepared by dissolving the required amount of $Zn(NO_3)_2 \cdot 6H_2O$ in DI water. Chemicals including 2,2-diphenyl-1-picrylhydrazyl (DPPH), methylene blue (MB), peptone, and sodium hydroxide were procured from Merck Chemicals, Mumbai, India. All reagents were of analytical grade and were used without further purification.

2.1 Collection of seaweed:

Samples were collected from shallow waters of the Gulf of Mannar region (Lat. 9◦17N Long. 79◦17E) at Mandapam, southeast coast of India. The collected seaweeds were washed with salt water to remove all the epiphytes and then allowed in distilled water for about 15 min to remove the salts. Thus, the collected seaweeds were air dried, then cut into small pieces and made Grind into powder and used for further studies. [20, 21]

2.2 Preparation of Seaweed Extract:

Gracilaria textorii red algae powder (5 g) was added to a conical flask containing 50 mL of ethanol. The mixture was vigorously stirred for two hours at 60°C. The extract was well filtered through Whatman filter paper then cooled and stored for the biosynthesis process.

2.3 Biosynthesis of zinc oxide nanoparticles:

The preparation of biosynthesis, 10 ml of seaweed leaf extract was added 90 ml of aqueous solution of 1 mM zinc nitrate. Then the solution was kept under constant stirring using a magnetic stirrer to completely dissolve the zinc nitrate. After complete dissolution of zinc nitrate, the flask containing the solution was heated on a water bath at 80°C for 5–10 min. The pH was adjusted between 5 and 10 using 0.1 M HCl or 0.1 M NaOH aqueous solution to the above aqueous solution and placed on magnetic stirrer for 1 h. Finally, the white precipitate was formed and used futher analysis. [22]

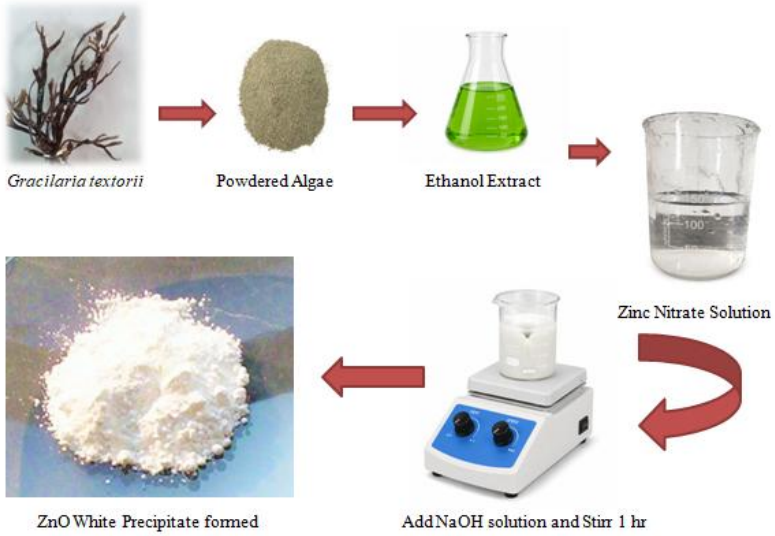

Figure 1. Synthesis of ZnO nanoparticles using Gracilaria textorii extract

3. CHARACTERISATION:

UV-Visible spectra analysis was performed on a JASCO V-650 UV - visible spectrophotometer. The XRD measurements were made by analytical X pert powder X Celerator Diffractometer, measurements range: 10 to 80 degree in 2θ and particle size was calculated using Scherrer's equation. The FT-IR spectra were recorded using a Nicolet iS5. The surface morphology of the nanoparticles was done using JEOL JSM-6700F. We conducted measurement using SEM & EDAX. The electrochemical analyser, CH Instruments Electrochemical Workstation model 650c was employed for various electrochemical studies.

REDVET - Revista electrónica de Veterinaria - ISSN 1695-7504
Vol 25, No. 1 (2024)
http://www.veterinaria.org
Article Received:25-02-2024 Revised: 10-03-2024 Accepted: 15-03-2024

3.1 Electrochemical Studies

The electrochemical performance of the biosynthesized ZnO nanoparticles was investigated using cyclic voltammetry (CV). The working electrode was fabricated by thoroughly mixing 70 wt% ZnO nanoparticles, 20 wt% graphite powder, and two drops of silicone oil as a binder to obtain a homogeneous paste. The resulting paste was uniformly coated onto a disk electrode surface. A platinum foil served as the counter electrode, while an Ag/AgCl electrode was employed as the reference electrode. Electrochemical measurements were carried out in 3 M KOH solution, which acted as the supporting electrolyte [23].

4. **Applications:**

4.1Photocatalytic Degradation of Methylene Blue (MB) Dye by ZnO Nanoparticles

The photocatalytic activity of the synthesized ZnO nanoparticles was evaluated through the degradation of methylene blue (MB) dye under natural sunlight irradiation. The experiment was performed using 100 mL of 20 ppm MB dye solution containing 50 mg of ZnO nanoparticles in a glass reactor. The reaction mixture was continuously stirred using a magnetic stirrer during the irradiation period. Prior to sunlight exposure, the suspension was maintained under dark conditions for 30 min to establish adsorption–desorption equilibrium between the dye molecules and the catalyst surface. At regular time intervals, aliquots of the reaction mixture were collected and centrifuged to remove the catalyst particles. The residual concentration of MB dye was determined by measuring the absorbance at 662 nm using a UV–Visible spectrophotometer. [24]

4.2 Antioxidant Activity of Synthesized CuO Nanoparticles

4.2.1 DPPH radical scavenging activity:

The antioxidant potential of the biosynthesized Zinc oxide nanoparticles was evaluated through their free radical scavenging ability against the stable 2,2-diphenyl-1-picrylhydrazyl (DPPH) radical assay [25,26]. Different concentrations of the synthesized nanoparticle algae extract (12.5, 25, 50, 100, and 200 µg/mL) were prepared and treated with 3.0 mL of 0.1 mM DPPH solution in methanol. The reaction mixtures were maintained in the dark at ambient temperature for 30 min. Subsequently, the absorbance was recorded at 517 nm using a UV–Vis spectrophotometer (Genesys 10S UV, Thermo Electron Corporation). Ascorbic acid served as the reference standard. The percentage inhibition of DPPH radicals was calculated using the following equation.

$$\% \text{ DPPH radical scavenging activity} = \frac{(A_0 - A_1)}{A_0} \times 100$$

Where A_0 is the absorbance of the control

A_1 is the absorbance of the test samples and reference.

All the tested samples were performed in triplicates and the results were averaged.

4.2.2 Hydrogen peroxide radial scavenging activity

As per the method [27, 28] Hydrogen peroxide (H_2O_2) scavenging ability of the synthesized nanoparticles ascorbic acid was established. In phosphate buffer (pH 7.4) a solution of H_2O_2 (40mM) was arranged. Dissimilar concentrations (12.5, 25, 50, 100 and 200 µg/mL) of nanoparticles ascorbic acid in 3.4 ml phosphate buffer were added. These are added to H_2O_2 solution (0.6 ml, 40 mM). At 230nm, the absorbance value of the reaction mixture was recorded. The percentage scavenging activity of H_2O_2 was determined using the following equation.

$$\text{Scavenging effect (\%)} = \frac{(A_0 - A_1)}{A_0} \times 100$$

Here A_0 is the absorbance of control and A_1 is the absorbance of the sample

4.3 Antibacterial activity

The test bacteria was inoculated in peptone water and incubated for 3 – 4 hours at 35 ºC. Mueller hinton agar plates was prepared and poured in sterile petriplates. 0.1 ml of bacterial culture was inoculated on the surface of Mueller hinton agar plates and spread by using L-rod. The inoculated plates were allowed to dry for five minutes. The disk loaded with samples concentration 1000 µg/ml was placed on the surface of inoculated petriplates using sterile technique. The plate was incubated at 37 ºC for 18-24 hours. The plate was examined for inhibitory zone and the zone of inhibition was measured in mm [29].

5. Result and Discussion:

5.1UV–Visible spectroscopy:

UV–Visible spectroscopy was employed to verify nanoparticle formation within the wavelength range of 200–800 nm. Earlier reports have shown that zinc oxide nanostructures typically display a characteristic absorption band between 350 - 380 nm [30]. The UV–Visible absorption spectrum obtained from the material synthesized using *Gracilaria textorii* extract is shown in Fig. 2. A prominent absorption maximum was observed at 374 nm, confirming the successful synthesis of the oxide nanomaterial [31]. The observed absorption arises from the excitation of electrons from the valence band to the conduction band, resulting in a characteristic electronic transition. The appearance of this

REDVET - Revista electrónica de Veterinaria - ISSN 1695-7504
Vol 25, No. 1 (2024)
http://www.veterinaria.org
Article Received:25-02-2024 Revised: 10-03-2024 Accepted: 15-03-2024

absorption feature in the ultraviolet region provides evidence for the formation of the nanoscale oxide particles. Furthermore, the optical properties of the synthesized material were investigated using the Tauc plot approach. The optical band gap energy was estimated according to the Tauc equation:

$$(\alpha h\nu)^2 = A\,(h\nu - Eg) \quad \ldots\ldots (1)$$

Where α is the absorption coefficient, hν is the photon energy, A is a constant, and Eg is the optical band gap energy. A plot of $(\alpha h\nu)^2$ versus photon energy (hν) was constructed, and the linear portion of the curve was extrapolated to the energy axis to determine the band gap value. [32] The band gap energy obtained from the Tauc plot was found to be approximately 3.3 eV, which is consistent with reported values for ZnO nanoparticles.

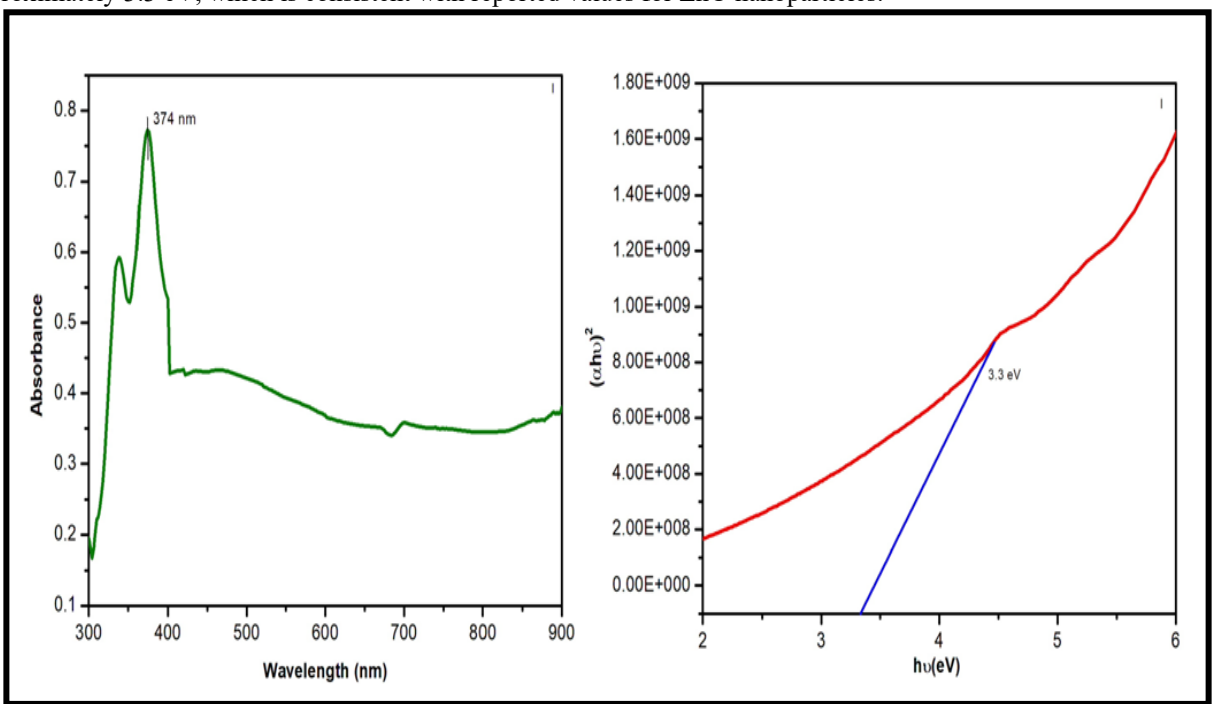

Figure. 2 (a) UV–Visible absorption spectrum of the synthesized ZnO nanoparticles using Gracilaria textorii extract and (b) Tauc plot used for the estimation of optical band gap energy

5.2 FTIR Analysis:

The FTIR spectrum of the synthesized zinc oxide nanoparticles using *Gracilaria textorii* algae extract was recorded in the range of 4000-500 cm-1 identify the functional group of the nanoparticles. Fig 3. A broad band observed around 3413 cm^{-1} is attributed to the O–H stretching vibration of hydroxyl groups [33], which may be due to absorbed water molecules or alcohol groups present in the *Gracilaria textorii* algae extract. The peak at 2924 cm^{-1} corresponds to C–H stretching vibrations of aliphatic groups present in biomolecules [34]. A weak band appearing at 2361 cm^{-1} is assigned to C≡C stretching vibrations [35]. The band observed at 1623 cm^{-1} is related to C=O stretching vibrations, indicating the presence of proteins and phenolic compounds from the algal extract that may participate in the reduction and stabilization of the nanoparticles. The peak at 1459 cm^{-1} is attributed to C–N stretching vibrations of aromatic amine groups [36]. In addition, the peak at 1048.37 cm^{-1} is assigned to the stretching vibration of the C–N bond of primary amines [37], while the band at 980 cm^{-1} corresponds to C–O stretching vibrations of alcohols, carboxylic acids, or polysaccharides. A strong absorption band observed at 618 cm^{-1} is characteristic of Zn–O stretching vibrations [38], confirming the formation of zinc oxide nanoparticles. The FTIR analysis indicates the presence of various phytochemicals such as polyphenols, proteins, and polysaccharides in the algal extract. These biomolecules may act as reducing and stabilizing agents during the synthesis process, while the presence of the Zn–O band confirms the successful formation of ZnO nanoparticles.

REDVET - Revista electrónica de Veterinaria - ISSN 1695-7504
Vol 25, No. 1 (2024)
http://www.veterinaria.org
Article Received:25-02-2024 Revised: 10-03-2024 Accepted: 15-03-2024

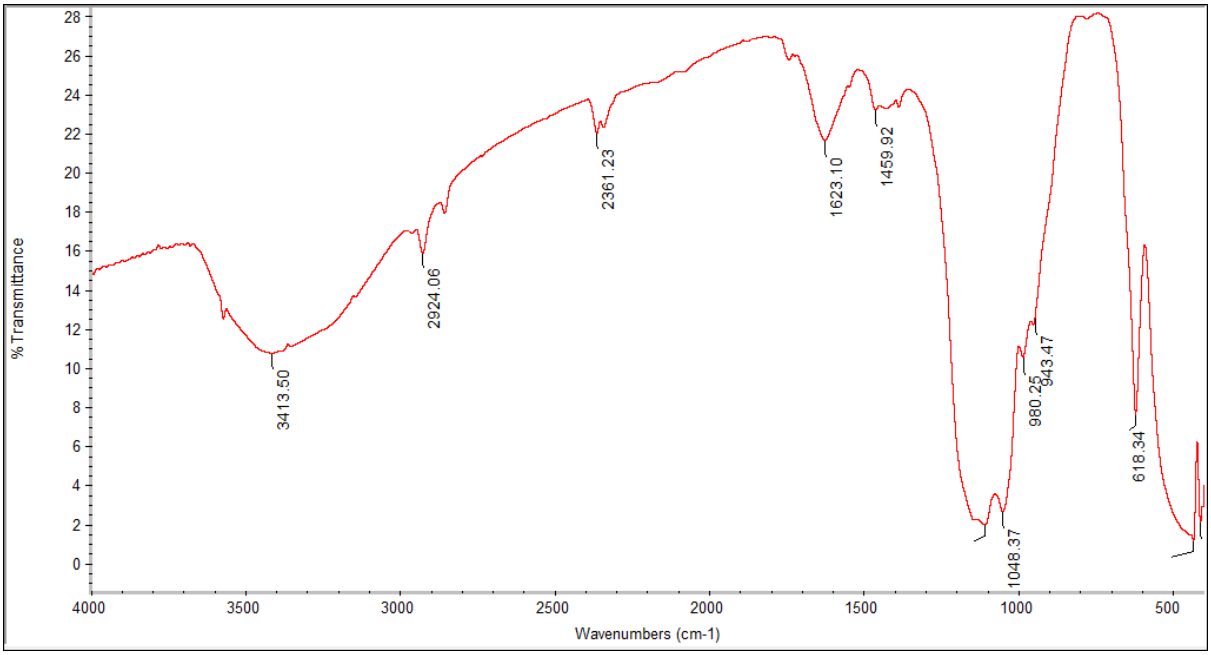

Figure 3. Fourier transform infrared (FTIR) spectrum of the synthesized zinc oxide nanoparticles using ethanol extract of *Gracilaria textorii*

5.3 XRD Analysis:

The Crystalline Structure and phase purity of ZnO nanoparticles synthesized using Gracilaria textorii extract were analyzed using X-ray diffraction. The XRD pattern Fig.4 exhibited well-defined diffraction peaks at 2θ values of approximately 31.779, 34.192, 36.624, 47.207, 56.563, 66.327, which correspond to the (100), (002), (101), (102), (110) and (201) planes,respectively. These diffraction peaks are in excellent agreement with the standard hexagonal wurtzite structure of ZnO, as reported in JCPDS Card No. 36-1451.[39] The absence of any additional impurity peaks indicates the high purity of the synthesized material. The average size of the ZnO nanoparticles was measured using the Debye-Scherrer equation [40]

$D = k\lambda \beta \cos\theta$ …….. (2)

where D is the average crystalline particle size, λ is the wavelength of x- ray (1.5406 Å), k is the shape factor or Scherer's constant (0.9), θ is Bragg's diffraction angle, and β is the XRD peak full width at half maximum. Using Scherrer's formula, the average crystalline size of the nano particles formed was estimated and found to be 34.8 nm. This confirms that the synthesized ZnO particles are in the nanometer range.

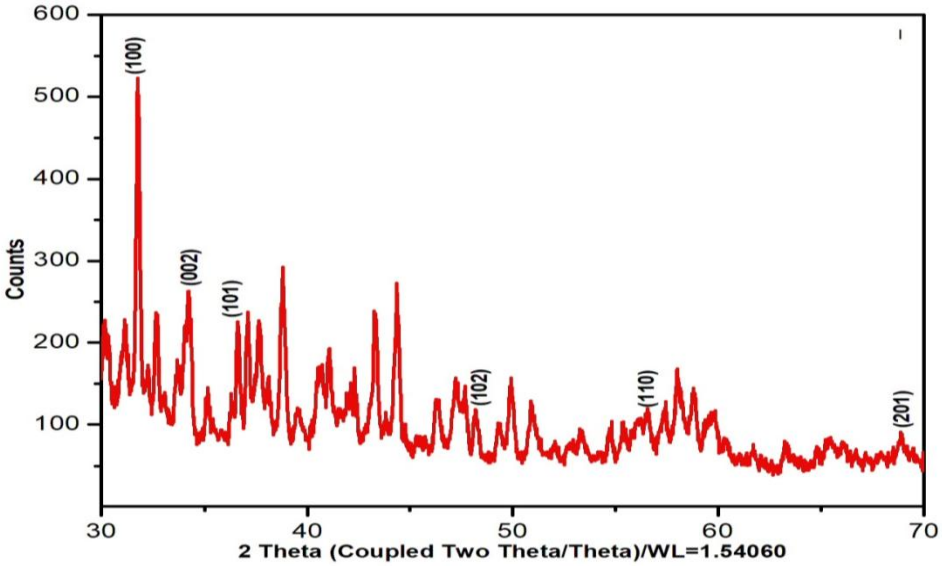

Figure. 4 XRD pattern of the synthesized ZnO nanoparticles through *Gracilaria textorii* extract

5.4 Scanning Electron Microscopic (FESEM) Analysis:

REDVET - Revista electrónica de Veterinaria - ISSN 1695-7504
Vol 25, No. 1 (2024)
http://www.veterinaria.org
Article Received:25-02-2024 Revised: 10-03-2024 Accepted: 15-03-2024

The scanning electron microscope (SEM) analysis was conducted to examine the shape and surface morphology of pure ZnO nanoparticles at different magnifications, and the findings are presented in Fig 5. The SEM images of ZnO nanoparticles synthesized a green method using extracts from *Gracilaria textorii* confirm the successful formation of stable nanoparticles. At a magnification of 20 µm, the SEM image shows that the ZnO nanoparticles possess a flake-like nanosheet structure with noticeable agglomeration. The particles appear irregularly distributed, forming a porous and layered arrangement, which is likely due to the role of biomolecules from the algae extract during the green synthesis process.

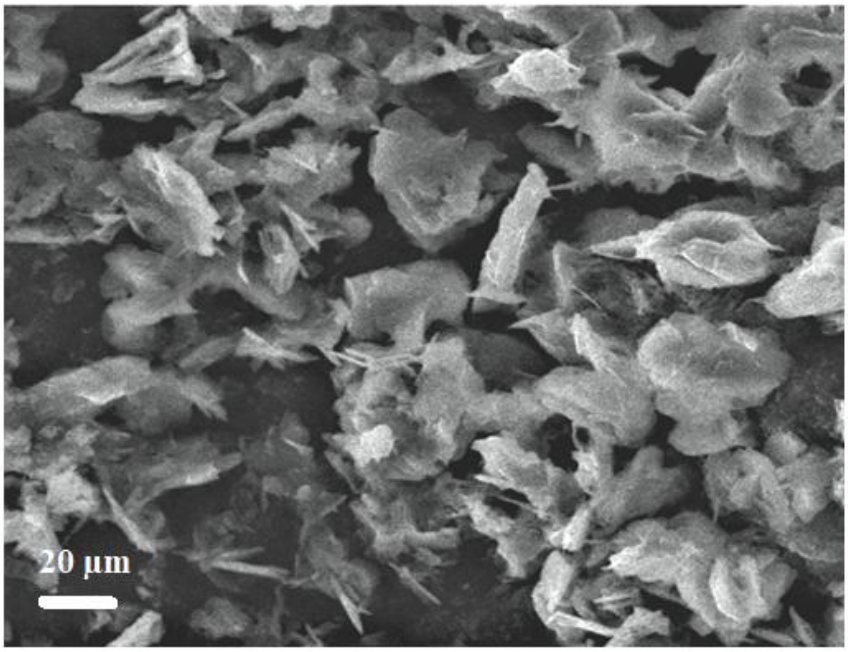

Figure. 5 SEM micrograph showing the surface morphology of the synthesized zinc oxide nanoparticles using algae extract

5.5 EDX analysis:

The elemental composition of the ZnO nanoparticles synthesized using *Gracilaria textorii* extract was confirmed through EDX analysis. The spectrum Fig.6 shows both peaks corresponding to zinc and oxygen, indicating the successful formation of ZnO nanoparticles. The atomic weight percentage of Zn and O to be 71.82% and 28.18%, respectively**.** Furthermore, the EDX spectrum displays a characteristic oxygen peak around 0.5 keV**,** along with zinc peaks observed at approximately 1 keV and 8.6 keV**.** The presence of minor variations in peak intensity may be attributed to residual phytochemical constituents derived from the algae extract used during synthesis.

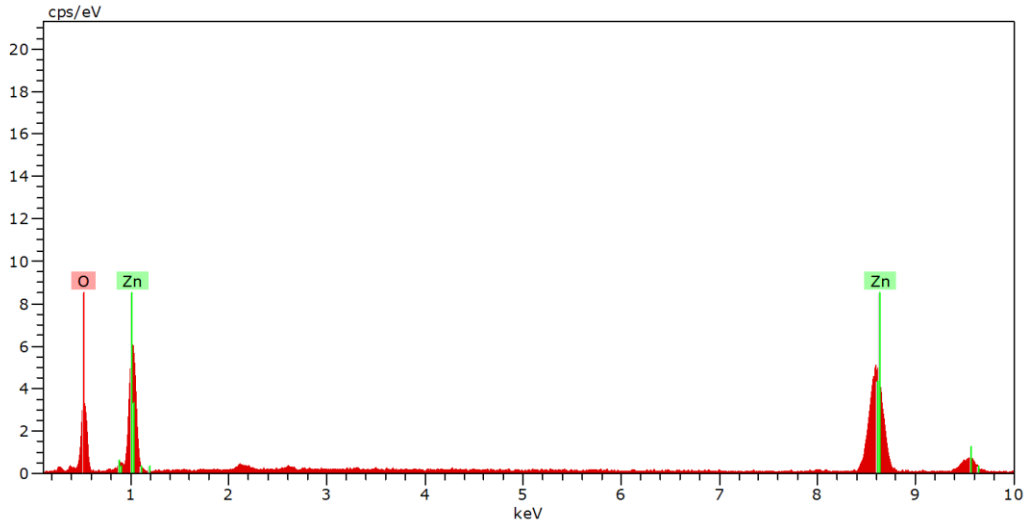

Figure.6 EDX analysis confirming the elemental composition of the synthesized zinc oxide nanoparticles

5.6 DLS Analysis:

REDVET - Revista electrónica de Veterinaria - ISSN 1695-7504
Vol 25, No. 1 (2024)
http://www.veterinaria.org
Article Received:25-02-2024 Revised: 10-03-2024 Accepted: 15-03-2024

The particle size distribution of ZnO nanoparticles synthesized using *Gracilaria textorii* extract was analyzed using DLS Fig 7. The results show a single peak with an average particle size of 2.8 nm, confirming nanoscale formation. The size distribution ranges from **1**–10 nm, with maximum intensity around 2–4 nm, indicating relatively uniform particle formation. The Z-average diameter was found to be 3838.3 nm, which is significantly higher than the mean size due to particle aggregation in the colloidal system. The polydispersity index (PDI) value of 0.351 indicates moderate size variation. Overall, the results confirm the successful synthesis of ZnO nanoparticles with slight agglomeration.

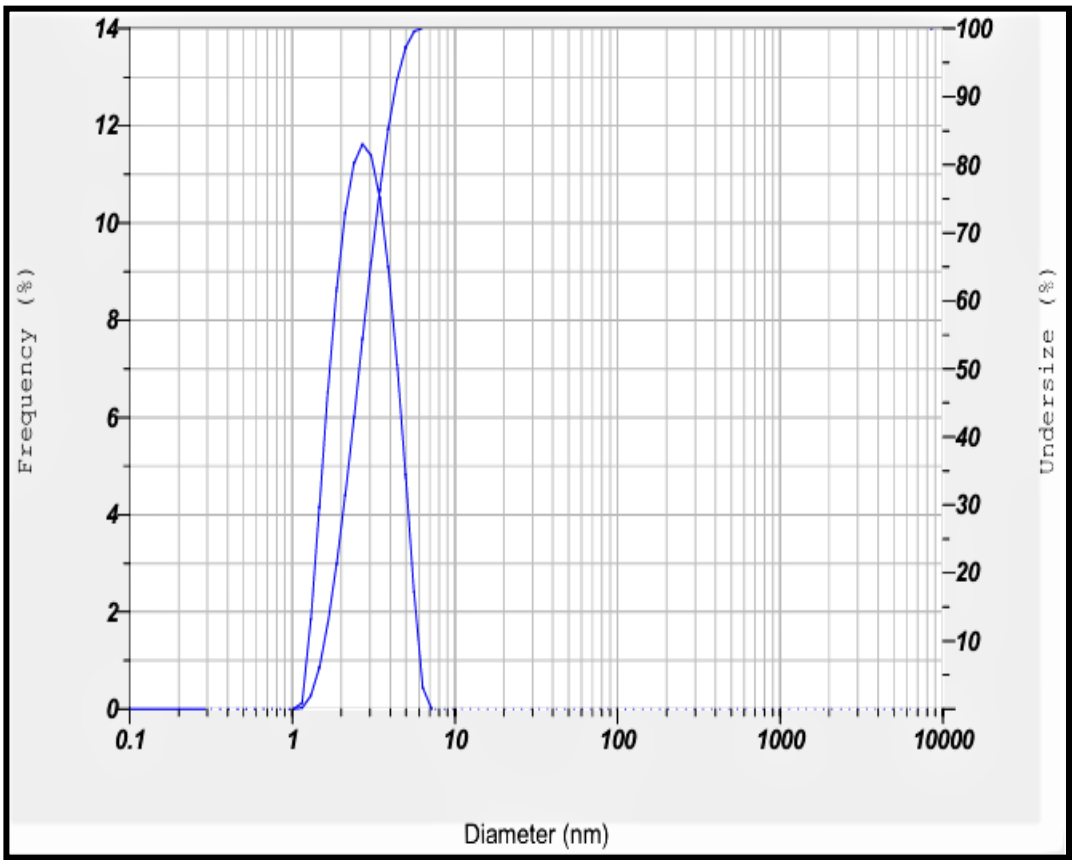

Figure. 7 DLS Spectra of ZnO NPs using Gracilaria textorii seaweed

5.7 Electrochemical Studies:

The electrochemical behavior of *Gracilaria textorii* mediated ZnO nanoparticles was evaluvate using cyclic voltammetry in a three-electrode configuration consisting of a glassy carbon working electrode, a platinum counter electrode, and an Ag/AgCl reference electrode. The analysis was performed in 3 M KOH electrolyte over a potential range of −0.8 to +0.4 V, with scan rates varying from 10 to 100 mV s^{-1} at room temperature. [41] The CV curves obtained at various scan rates are shown in Fig 8. shows exhibited a quasi-rectangular shape with broad anodic and cathodic regions, indicating the combined contribution of electric double-layer capacitance and surface redox reactions associated with ZnO nanoparticles. As the scan rate increased from 10 to 100 mV s^{-1}, the enclosed area of the curves gradually increased, accompanied by a corresponding rise in anodic and cathodic current densities. This behavior demonstrates the good electrochemical reversibility and rapid charge-transfer kinetics of the synthesized ZnO nanoparticles. Similar observations have been reported for green-synthesized ZnO nanomaterials employed in supercapacitor applications [42]. The increase in current response with scan rate further suggests efficient charge-transfer kinetics and rapid ion diffusion at the electrode–electrolyte interface. These characteristics are commonly associated with pseudocapacitive materials and demonstrate the ability of the biosynthesized ZnO nanoparticles to maintain their electrochemical performance under varying operating conditions.

REDVET - Revista electrónica de Veterinaria - ISSN 1695-7504
Vol 25, No. 1 (2024)
http://www.veterinaria.org
Article Received:25-02-2024 Revised: 10-03-2024 Accepted: 15-03-2024

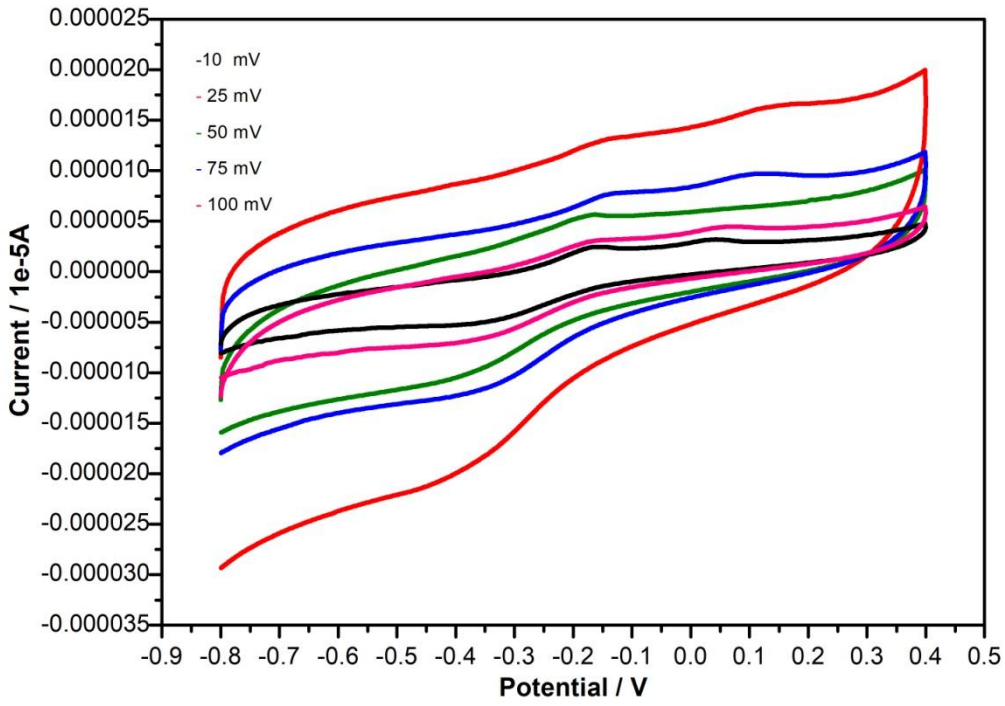

Figure.8 Cyclic volatametry of Zinc oxide nanoparticles using 3M KOH

Fig. 9 illustrates the effect of scan rate on the anodic (Ipa) and cathodic (Ipc) peak currents of the biosynthesized ZnO nanoparticles. A steady increase in both peak currents was observed as the scan rate increased from 10 to 100 mV s^{-1}, indicating improved electrochemical responsiveness of the material. The anodic current increased from approximately 4.3 mA to 24.5 mA, while the cathodic current increased from −2.8 mA to −16.0 mA. The enhanced current values at higher scan rates suggest rapid electron transport and effective charge-transfer processes at the electrode surface. The results further reveal efficient utilization of electroactive sites and favorable ion diffusion within the electrode–electrolyte interface. The synthesized ZnO nanoparticles using *Gracilaria textorii* extract exhibited excellent electrochemical characteristics and their suitability for energy-storage and supercapacitor applications [43].

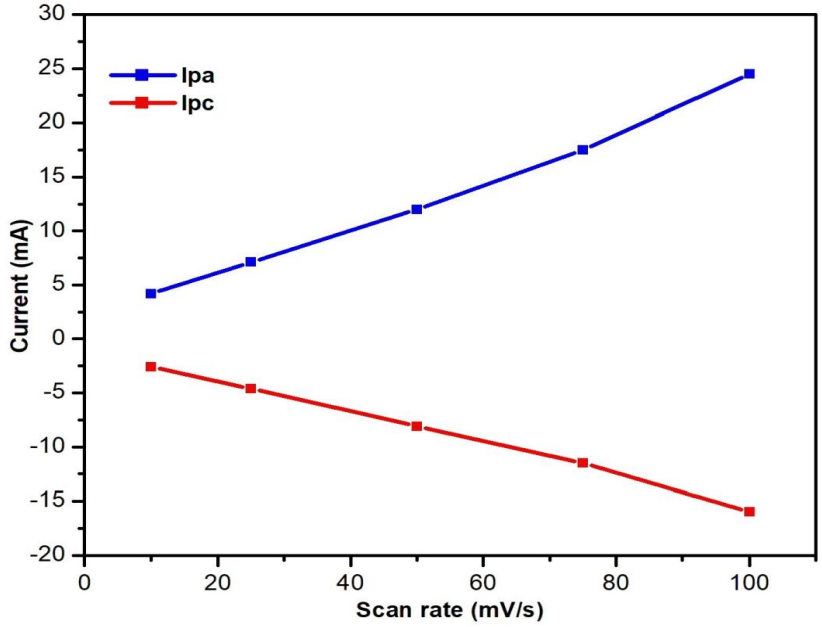

Figure.9 Plot of Current Vs Scan rate ZnO NPs using *Gracilaria textorii* extract

REDVET - Revista electrónica de Veterinaria - ISSN 1695-7504
Vol 25, No. 1 (2024)
http://www.veterinaria.org
Article Received:25-02-2024 Revised: 10-03-2024 Accepted: 15-03-2024

6. APPLICATIONS:

6.1 Photocatalytic Degradation of MB Dye:

The photocatalytic activity of the biosynthesized ZnO nanoparticles was assessed by monitoring the degradation of methylene blue (MB) dye under sunlight irradiation using UV–Visible spectroscopy. As illustrated in Fig. 10(a) the absorption spectra recorded at different irradiation times (0–70 min) exhibited a distinct absorption band centered at approximately 662 nm, which is characteristic of MB dye. A progressive decline in absorbance intensity was observed with increasing irradiation time, demonstrating the effective degradation of the dye molecules. The maximum absorbance was recorded before irradiation (0 min), whereas a substantial reduction in peak intensity was noted after 70 min of exposure, confirming the photocatalytic efficiency of the synthesized ZnO nanoparticles. This decrease in absorbance can be attributed to the breakdown of the chromophoric structure of MB during the photocatalytic process. Fig.10 (b) The degradation efficiency was calculated, and approximately 76% of the methylene blue dye was degraded within 70 minutes**,** confirming the strong photocatalytic activity of ZnO nanoparticles. A comparable degradation efficiency of 78.3% was reported for green-synthesized ZnO nanocrystals [44], while observed approximately 74% degradation using ZnO nanoparticle thin films.[45] The slight differences in degradation efficiency may be attributed to variations in synthesis method, particle size, morphology, catalyst dosage, irradiation source, and reaction conditions.
The percentage of dye degradation is calculated according to equation (3)

$$\%\ Degradation = \frac{(C_0 - C_t)}{C_0} \times 100 \qquad \ldots\ldots (3)$$

Where Co = initial concentration of dye before exposure to visible light irradiation,
Ct = concentration of dye at a specific time t

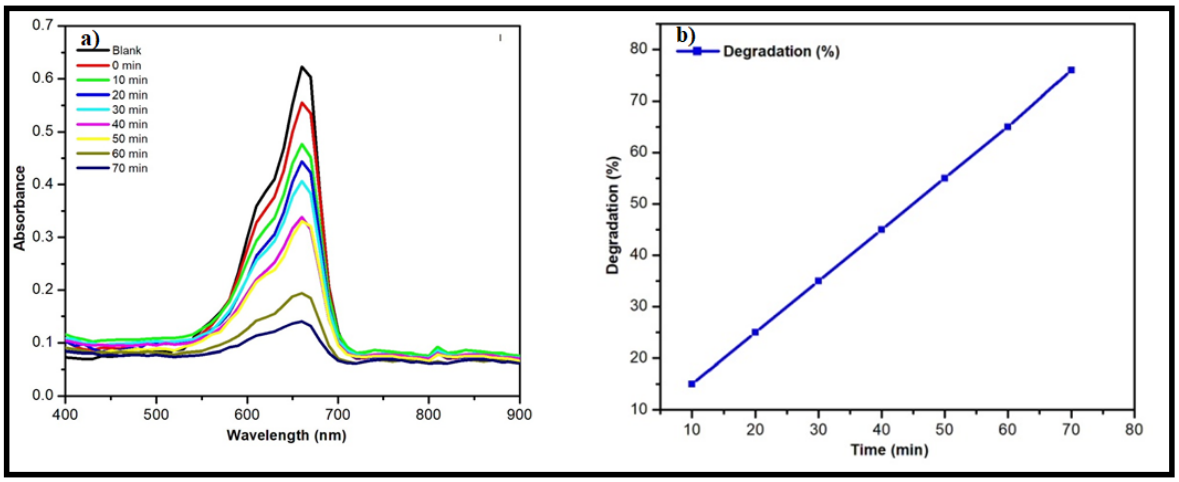

Figure. 10 UV–Vis absorption spectra of photocatalytic degradation of methylene blue using seaweed extract

6.2 Photocatalytic Mechanism of ZnO Nanoparticles

The photocatalytic degradation of methylene blue (MB) dye by ZnO nanoparticles under sunlight irradiation is governed by the generation of reactive oxygen species through a photo induced redox process. Fig.11 ZnO is a wide-band-gap semiconductor that can absorb photons with energy equal to or greater than its band-gap energy. Upon light irradiation, electrons in the valence band are excited to the conduction band, leaving behind positively charged holes in the valence band. The formation of these electron–hole pairs initiates a series of oxidation and reduction reactions on the surface of the photocatalyst.The photogenerated electrons migrate to the surface of the ZnO nanoparticles and react with dissolved oxygen molecules to form superoxide radical anions ($\bullet O_2^-$). Simultaneously, the holes react with adsorbed water molecules or hydroxide ions to produce hydroxyl radicals (•OH). These reactive oxygen species are highly oxidative and play a critical role in the degradation of organic pollutants.[46,47]

$ZnO + h\nu \rightarrow ZnO\ (e^-) + ZnO\ (h^+)$

$ZnO\ (e^-) + O_2 \rightarrow ZnO + \bullet O_2^-$

$ZnO\ (h^+) + H_2O \rightarrow ZnO + \bullet OH + H^+$

$H^+ + \bullet O_2^- \rightarrow \bullet OOH$

$\bullet OOH + \bullet OOH \rightarrow H_2O_2 + O_2$

$ZnO\ (e^-) + H_2O_2 \rightarrow ZnO + \bullet OH + OH^-$

REDVET - Revista electrónica de Veterinaria - ISSN 1695-7504
Vol 25, No. 1 (2024)
http://www.veterinaria.org
Article Received:25-02-2024 Revised: 10-03-2024 Accepted: 15-03-2024

$MB + \bullet O_2^-/\bullet OH/h^+ \rightarrow$ Intermediates $\rightarrow CO_2 + H_2O$

The generated superoxide and hydroxyl radicals attack the chromophoric structure of methylene blue molecules adsorbed on the catalyst surface. The continuous oxidative degradation leads to the cleavage of aromatic rings, demethylation, and the breakdown of intermediate compounds into smaller molecular fragments. As the reaction progresses, these intermediates undergo further oxidation and are ultimately converted into environmentally benign products such as carbon dioxide, water, and inorganic ions. Furthermore, sunlight irradiation promotes the continuous generation of electron–hole pairs, sustaining the photocatalytic process throughout the reaction period. The gradual decrease in the characteristic absorption intensity of methylene blue observed in UV–Vis spectra confirms the successful degradation of the dye and demonstrates the effectiveness of ZnO nanoparticles as photocatalysts for wastewater remediation applications.

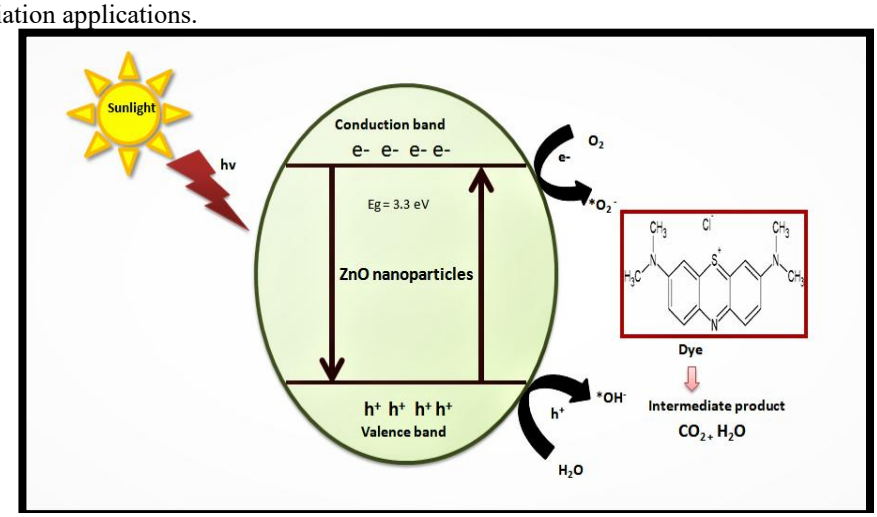

Figure.11 Photocatalytic degradation of Mechanism of ZnO NPs

6.2.1 PSEUDO FIRST ORDERS KINETICS:

The degradation efficiency of methylene blue (MB) was studied by varying the amount of photocatalyst and the kinetics were analyzed based on a pseudo-first-order model.

The photocatalytic reaction follows the kinetic expression:

$$ln\left(\frac{C0}{Ct}\right) = kt \ldots\ldots (4)$$

Where C_0 represents the initial dye concentration, Ct represents the dye concentration at time *t*, and *k* is the apparent rate constant (min^{-1}). [48] The linear plot of ln (C*0*/C*t*) versus irradiation time Fig.12 confirms that the degradation process follows pseudo-first-order kinetics. The rate constant (k) was calculated from the slope of the linear regression plot. The obtained rate constant was 0.0123 min^{-1}, and the correlation coefficient (R^2) was 0.9931. The high R^2 value indicates excellent linearity and strong agreement with the pseudo-first-order kinetic model, thereby confirming the efficient photocatalytic performance of the synthesized ZnO nanoparticles.

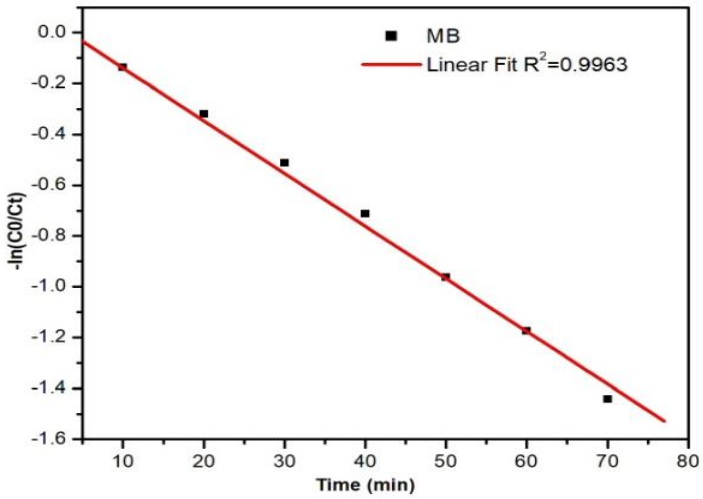

Figure. 12 Pseudo First order kinetics of MB dye Synthesized from *Gracilaria textorii*

REDVET - Revista electrónica de Veterinaria - ISSN 1695-7504
Vol 25, No. 1 (2024)
http://www.veterinaria.org
Article Received:25-02-2024 Revised: 10-03-2024 Accepted: 15-03-2024

6.3 Antioxidant activity of ZnO Nanoparticles:

6.3.1 DPPH Assay:

The antioxidant activity of ZnO nanoparticles synthesized using Gracilaria textorii was assessed through the DPPH radical scavenging assay, and the corresponding results are illustrated in Figure 13 (a) The DPPH scavenging activity of both ZnO nanoparticles and ascorbic acid increased progressively with increasing concentration (25–125 µg/mL), indicating a concentration-dependent antioxidant behavior. The DPPH scavenging activity of ZnO nanoparticles increased from 11.48 ± 0.11% at 25 µg/mL to 62.76 ± 0.23% at 125 µg/mL. Similarly, ascorbic acid exhibited scavenging activities ranging from 13.28 ± 0.12% to 66.72 ± 0.21% within the same concentration range. At all tested concentrations, the standard antioxidant showed slightly higher scavenging activity than the ZnO nanoparticles. However, the synthesized nanoparticles demonstrated substantial antioxidant capacity, particularly at higher concentrations. Fig 13 (b) The IC_{50} value of the ZnO nanoparticles was determined to be 82.16 µg/mL, whereas the standard Ascorbic acid exhibited a lower IC_{50} value of 78.22 µg/mL, suggesting its comparatively higher antioxidant efficiency. These findings are consistent with recent reports on seaweed- and plant-derived ZnO nanoparticles exhibiting notable antioxidant properties.[49] However, the small difference between the IC_{50} values indicates that the ZnO nanoparticles synthesized using Gracilaria textorii possess notable free radical scavenging capability.[50] The observed antioxidant activity can be attributed to the presence of bioactive constituents such as phenolic and flavonoid compounds derived from *Gracilaria textorii*, which function as both reducing and stabilizing agents during nanoparticle formation [51]. These phytochemicals are known to enhance the electron-donating capacity of the nanoparticles, thereby facilitating the effective neutralization of DPPH free radicals [52]. The results confirm that the synthesized ZnO nanoparticles exhibit significant antioxidant potential and are effective in scavenging DPPH radicals.

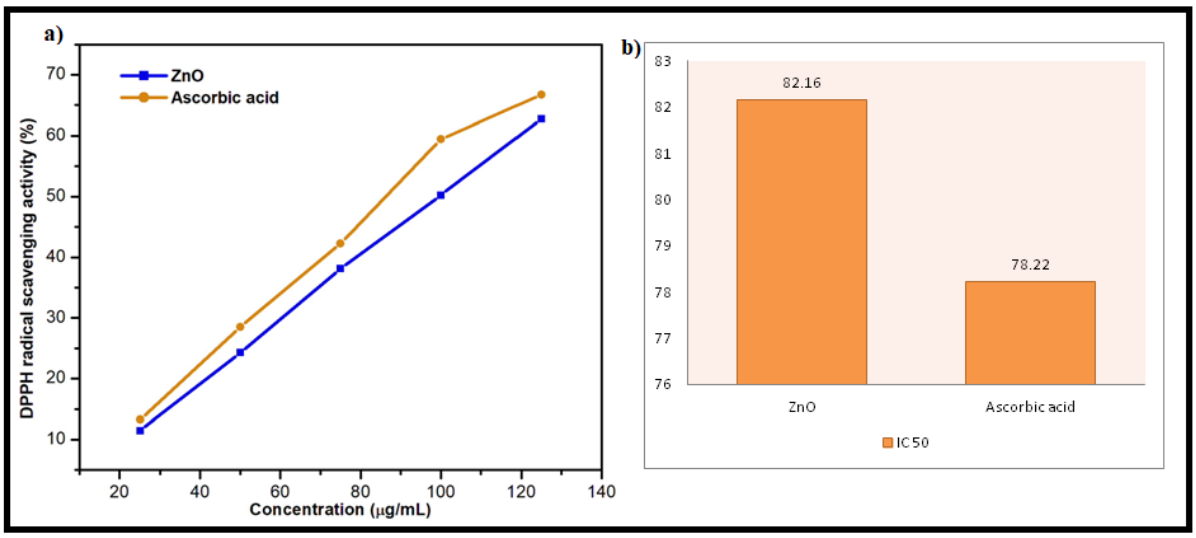

Figure .13 (a) DPPH radical Scavenging activity (b) IC50 value of ZnO NPs using red algae

6.3.2 Hydrogen peroxide radical assay:

The hydrogen peroxide (H_2O_2) scavenging activity of ZnO nanoparticles synthesized using *Gracilaria textorii* extract was evaluated over a concentration range of 25–125 µg/mL and compared with the standard antioxidant, ascorbic acid. The antioxidant activity determined by the H_2O_2 radical scavenging assay is presented in Fig. 14(a) The results revealed a concentration-dependent increase in scavenging activity for both the synthesized ZnO nanoparticles and the standard antioxidant. At lower concentrations, the ZnO nanoparticles exhibited lower scavenging activity than ascorbic acid. However, a significant increase in antioxidant activity was observed with increasing concentration. The percentage inhibition increased progressively from the lowest to the highest concentration, indicating enhanced hydrogen peroxide scavenging efficiency of the synthesized nanoparticles. It was observed that the ZnO nanoparticles exhibited slightly higher scavenging activity at 100 µg/mL, whereas at 125 µg/mL, the inhibition efficiencies of the nanoparticles and ascorbic acid were nearly comparable. Fig 14(b) The IC_{50} values, representing the concentration required to scavenge 50% of hydrogen peroxide radicals, were determined to be 74.48 µg/mL for the ZnO nanoparticles and 71.32 µg/mL for ascorbic acid. Although the standard antioxidant exhibited a slightly lower IC_{50} value, indicating greater antioxidant effectiveness, the relatively close IC_{50} values suggest that the synthesized ZnO nanoparticles possess considerable hydrogen peroxide scavenging activity.

REDVET - Revista electrónica de Veterinaria - ISSN 1695-7504
Vol 25, No. 1 (2024)
http://www.veterinaria.org
Article Received:25-02-2024 Revised: 10-03-2024 Accepted: 15-03-2024

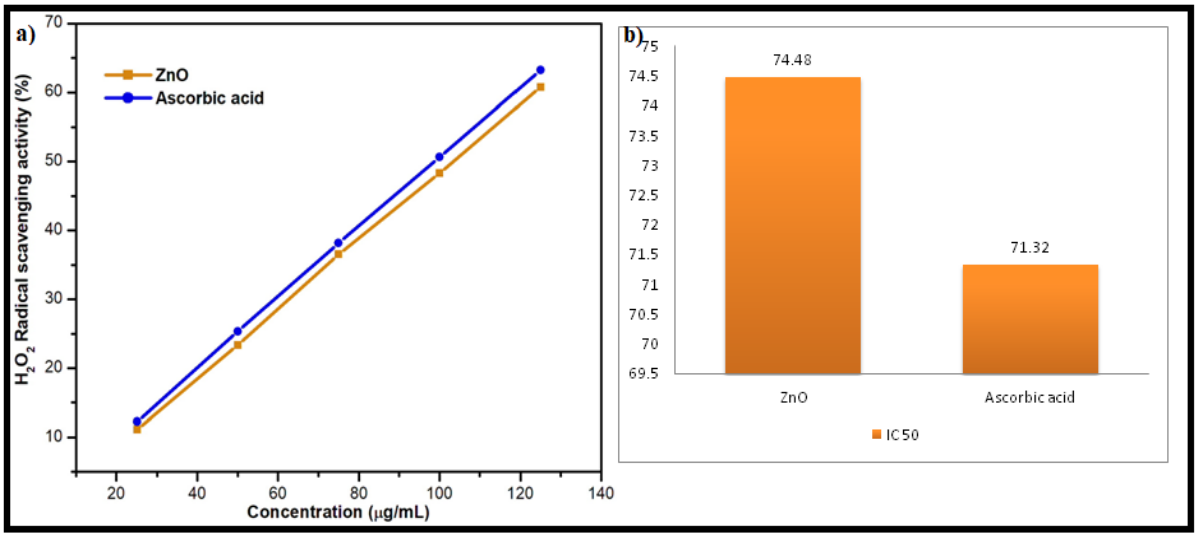

Figure .14 (a) Hydrogen peroxide (H_2O_2) scavenging activity of ZnO nanoparticles (b) IC50 value of ZnO NPs using *Gracilaria textorii*

6.4 Antibacterial activity:

The antibacterial activity of ZnO nanoparticles synthesized using *Gracilaria textorii* extract was assessed against *Escherichia coli*, *Staphylococcus aureus*, and *Pseudomonas aeruginosa* using the agar well diffusion method. The results presented in Fig.15 (a&b) and Table 1 demonstrates that the synthesized ZnO nanoparticles exhibited appreciable antibacterial activity against all tested bacterial strains. The standard antibiotic ciprofloxacin produced inhibition zones of 27 mm against *E. coli* and 25 mm against both *S. aureus* and *P. aeruginosa*, indicating its superior antibacterial efficacy. However, ZnO nanoparticles also demonstrated noticeable inhibitory effects, with the zone of inhibition generally increasing as the nanoparticle concentration increased.

Among the tested organisms, *P. aeruginosa* showed the highest susceptibility toward ZnO nanoparticles, with inhibition zones increasing from 15 mm at 50 µL to 20 mm at 150–250 µL. Similarly, *S. aureus* exhibited significant antibacterial activity, showing a maximum inhibition zone of 19 mm at 250 µL. In contrast, *E. coli* displayed comparatively lower sensitivity, with inhibition zones ranging from 7 mm to 15 mm. The lower susceptibility of *E. coli* may be attributed to the complex outer membrane structure of Gram-negative bacteria, which acts as an additional barrier against nanoparticle penetration. The antibacterial efficacy of the ZnO nanoparticles can be attributed to their nanoscale dimensions and high surface area, which facilitate strong interactions with bacterial cell membranes. The bioactive constituents present in *Gracilaria textorii* extract, including phenolic compounds, polysaccharides, and other secondary metabolites, are believed to play a significant role in the stabilization of ZnO nanoparticles and may positively influence their biological properties [53]. The results obtained in the present study reveal that the synthesized ZnO nanoparticles exhibit effective antibacterial activity against both Gram-positive and Gram-negative bacterial strains. The broad-spectrum antimicrobial efficacy observed highlights the potential of these nanoparticles as sustainable and eco-friendly materials for future biomedical and pharmaceutical applications.

Table.1 Antibacterial activity of ZnO nanoparticles using Gracilaria textorii ethanol extract:

Bacteria	Inhibition zone in mm					
	Ab ciprofloxacin	50 µl	100 µl	150 µl	200 µl	250 µl
E.coli	27	7	12	15	15	15
Staphylococcus aureus	25	15	16	18	15	19
Pseudomonas aeruginosa	25	15	17	20	20	20

REDVET - Revista electrónica de Veterinaria - ISSN 1695-7504
Vol 25, No. 1 (2024)
http://www.veterinaria.org
Article Received:25-02-2024 Revised: 10-03-2024 Accepted: 15-03-2024

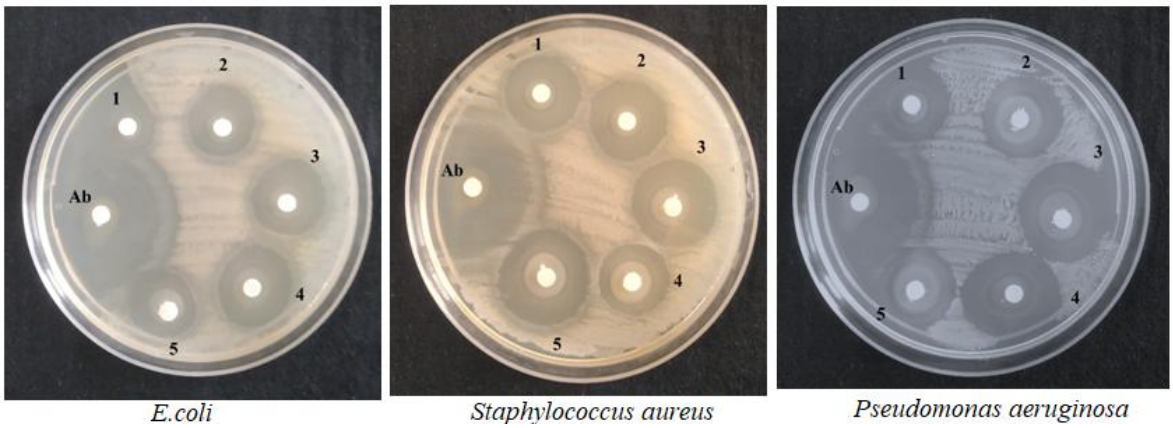

Figure 15 (a). Antibacterial activity of ZnO nanoparticles using ethanol extract of algae using the agar well diffusion method

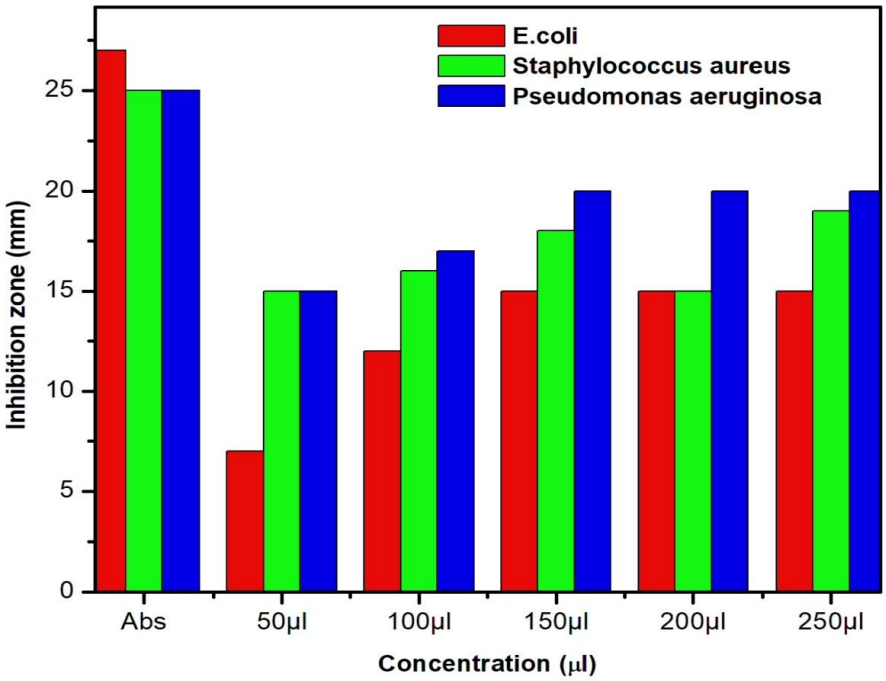

Figure 16 (b) Bar diagram of agar well diffusion method using ZnO nanoparticles

7. Conclusion:

In the present study, ZnO nanoparticles were fabricated using *Gracilaria textorii* extract through a green synthesis strategy that avoids the use of hazardous chemicals. The bioactive compounds present in the algae extract played a crucial role in the reduction and stabilization of the nanoparticles. Comprehensive characterization by UV–Vis, FTIR, XRD, SEM, EDX, and DLS analyses verified the formation, crystallinity, morphology, elemental composition, and particle size distribution of the synthesized ZnO NPs. Electrochemical investigations using cyclic voltammetry demonstrated enhanced electron-transfer behavior, indicating the suitability of the nanoparticles for catalytic applications. The photocatalytic activity of the synthesized ZnO NPs was assessed against methylene blue (MB) dye under light irradiation. A continuous decline in the characteristic absorption peak of MB was observed with increasing irradiation time, and significant decolorization was achieved after 70 min, confirming the efficient photocatalytic performance of the nanoparticles. Moreover, the ZnO NPs exhibited pronounced antibacterial efficacy against *Escherichia coli, Staphylococcus aureus, and Pseudomonas aeruginosa*. The nanoparticles also showed considerable free-radical scavenging potential in both DPPH and H_2O_2 antioxidant assays. Overall, the results demonstrate that algae-mediated ZnO nanoparticles possess promising photocatalytic, antibacterial, and antioxidant properties, making them attractive candidates for environmental and biomedical applications.

REDVET - Revista electrónica de Veterinaria - ISSN 1695-7504
Vol 25, No. 1 (2024)
http://www.veterinaria.org
Article Received:25-02-2024 Revised: 10-03-2024 Accepted: 15-03-2024

ACKNOWLEDGMENT:
I acknowledge the PG & Research Department of Chemistry, A.P.C. Mahalaxmi College for Women, Thoothukudi, for providing laboratory for synthesis nanoparticles and study for photocatalytic degradation, UV & FTIR Study V.O.Chidambaram college PG& Research Department of chemistry, Thoothukudi, XRD and Cyclic voltammetry study Avinashlingam Institute for the Home Science and Higher education for Women, Coimbatore, Tamilnadu, and Gandhigram Rural Institute, Dindigul, Tamilnadu, India, study for SEM & EDAX. Antioxidant activity study BIOmelTez Research & Development Pvt Ltd, Kanyakumari. Antibacterial studies from kamaraj college, Thoothukudi.

CONFLICT OF INTEREST:
The authors declare no conflict of interest.

FUNDING DECLARATION:
There was no funding declaration

ETHICS DECLARATION:
Not applicable

REFERENCE:
1. Krause, M. (2014) Introduction to Nanotechnology, supported by VERITOX ser vices,Toxicology and Industrial Hygiene. https://www.aiha.org/aihce07/handouts/rt201krause.pd
2. Albrecht MA, Evan CW, Raston CL: Green chemistry and the health implications of nanoparticles. Green Chem 2006, 8:417–432.
3. Ananthu C Mohana, Renjanadevi B (2015)., Preparation of Zinc Oxide Nanoparticles and its Characterization Using Scanning Electron Microscopy (SEM) and X-Ray Diffraction (XRD). International Conference on Emerging Trends in Engineering, Science and Technology (ICETEST-2015). Procedia Technology. DOI: http://dx.doi.org/doi:10.1016/j.protcy.2016.05 .078. 24. 761 – 766.
4. Luo J, Wang Y, Zhang Q. Progress in perovskite solar cells based on ZnO nanostructures. Sol Energy. 2018;163:289-306
5. Nawaz, H.R., Solangi, B.A., Zehra, B. and Nadeem, U. (2011) Preparation of Nano Zinc Oxide and Its Application in Leather as a Retanning and Antibacterial Agent. Canadian Journal on Scientific and Industrial Research, 2, 164-170
6. Sokovnin SY, Il'ves VG, Khrustov VR, Zuev MG. Investigation of properties of ZnO ceramics sintered from ZnO-Zn nanopowders produced by pulsed electron beam evaporation. Ceram Int. 2017;43(14):10637-44.
7. Haq, A.N.U., Nadhman, A., Ullah, I., Mustafa, G., Yasinzai, M. and Khan, I. (2017) Synthesis Approaches of Zinc Oxide Nanoparticles: The Dilemma of Ecotoxicity. Journal of Nanomaterials, 2017, 1-14. https://doi.org/10.1155/2017/8510342
8. Tamer, T. M., Abou-Taleb, W. M., Roston, G. D., Mohyeldin, M. S., Omer, A. M. and Hafez, A. M. (2018)., Formation of Zinc Oxide Nanoparticles Using Alginate as a Template for Purification of Waste Water. Environmental Nanotechnology, Monitoring and Management. DOI: https://doi.org/10.1016/j.enmm.2018.04.006. 112 – 121.
9. Raha, S. and Ahmaruzzaman, M. (2022)., ZnO nanostructured materials and their potential applications: progress, challenges and perspectives. Nanoscale Advances. DOI: 10.1039/d1na00880c. 4, 1868-1925
10. Vigneshwaran N, Kumar S, Varadarajan PV, Prasad V: Functional finishing of cotton fabrics using Zinc oxide soluble starch nano composites. Nanotechnology 2006, 17:5087–5095.
11. Agarwal H, Kumar SV, Rajeshkumar S: A review on green synthesis of zinc oxide nanoparticles–An eco-friendly approach. Resour. Technol. 2017; 3: 406–413
12. Shinwari ZK, Maaza M: The study of structural, physical and electrochemical activity of Zno nanoparticles synthesized by green natural extracts of sageretia thea. Arch. Med. 2017; 3:9
13. Chandran, P. R., Naseer, M., Udupa, N., & Sandhyarani, N. (2011). Size controlled synthesis of biocompatible gold nanoparticles and their activity in the oxidation of NADH. Nanotechnology, 23(1), 015602. https://doi.org/10.1088/0957- 4484/23/1/015602
14. Smit, A.J. Medicinal and pharmaceutical uses of seaweed natural products: A review. J. Appl. Phycol. 2004, 16, 245–262.
15. Subhash RY, Uday NH, Bhupal BC. Therapeutic potential and health benefits of Sargassum species. Pharmacogn Rev. 2014;8(15):1–7.
16. Adl SM, Simpson AGB, Farmer MA et al. (2005) The new higher level classification of eukaryotes with emphasis on the taxonomy of protests. Journal of Eukaryotic Microbiology 52: 399–451.
17. Lee, R.E. (2008). *Phycology* (4th ed.). Cambridge University Press. ISBN 978-0-521-63883-8
18. Kim, S. K., & Wijesekara, I. (2010). Development and biological activities of marinederived bioactive peptides: A review. Journal of Functional Foods, 2, 1–9.[5]

19. Roseline, Thynraj Antony, Muthiyal Prabakaran Sudhakar, and Kulanthaiyesu Arunkumar. "Aqueous extraction of red seaweed bioactive compounds and synthesis of silver nanoparticles for agriculture applications." *Journal of Agriculture and Food Research* 14 (2023): 100769.
20. Kanaan, H.; Belous, O. *Marine Algae of the Lebanese Coast*; Nova Science Publishers: New York, NY, USA, 2016; pp. 1–126. ISBN 978-1-53610-211-6.
21. Nagarajan, Sangeetha, and Kumaraguru Arumugam Kuppusamy. "Extracellular synthesis of zinc oxide nanoparticle using seaweeds of gulf of Mannar, India." *Journal of nanobiotechnology* 11.1 (2013): 39.
22. Vanaja M, Paulkumar K, Baburaja M, Rajeshkumar S, Gnanajobitha G, Malarkodi C, et al. Degradation of methylene blue using biologically synthesized silver nanoparticles. Bioinorg Chem Appl 2014; 10:1-8.
23. Nagaswarupa, H. P., Mylarappa, M., Siddeswara, D. M. K., Mahesh, K. R. V., & Raghavendra, N. (2018). Fabrication and hierarchical structure of ZnO nanoparticles using green fuels: Cyclic voltammetry and impedance analysis. *Materials Today: Proceedings, 5*(10), 22547–22553. https://doi.org/10.1016/j.matpr.2018.06.602
24. Pai, S., Sridevi, H., Varadavenkatesan, T., Vinayagam, R., & Selvaraj, R. (2019). Photocatalytic zinc oxide nanoparticles synthesis using *Peltophorum pterocarpum* leaf extract and their characterization. *Optik, 185*, 248–255. https://doi.org/10.1016/j.ijleo.2019.03.174
25. Blois, M. S.(1958) "Antioxidant Determination by the Use of a Stable Free Radical." *Nature* 181 : 1199–1200. https://doi.org/10.1038/1811199a0.
26. Makvana, C., F. Arodiya, and K. Parmar.(2021) "Green Synthesis of Polymer-Capped Copper Nanoparticles Using *Ocimum sanctum* Leaf Extract: Antibacterial and Antioxidant Potential." *Bioscience Biotechnology Research Communications* 14 : 1832–1838. http://dx.doi.org/10.21786/bbrc/14.4.67.
27. Revathi, S. L., S. Kumar, V. Sudarshana Deepa, and S. Kumar. (2014) "Antimicrobial Activity of *A. serphyllifolia* (Rohl ex. Vow) Wright." *International Journal of Pharmaceutical Health Care Research* : 2249–2257.
28. Ramasamy, P., N. Subhapradha, V. Shanmugam, and A. Shanmugam.(1885) "Extraction, Characterization and Antioxidant Property of Chitosan from Cuttlebone *Sepia kobiensis* ." *International Journal of Biological Macromolecules* 64 (2014): 202–212. https://doi.org/10.1016/j.ijbiomac.2013.12.017.
29. Bauer, A. W., W. M. M. Kirby, J. C. Sherris, and M. Turck.(1966) "Antibiotic Susceptibility Testing by a Standardized Single Disk Method." *American Journal of Clinical Pathology* 45, no. 4 : 493–496. https://doi.org/10.1093/ajcp/45.4_ts.493.
30. Alyamani, A. A., Albukhaty, S., Aloufi, S., AlMalki, F. A., Al-Karagoly, H., & Sulaiman, G. M. (2021). Green fabrication of zinc oxide nanoparticles using phlomis leaf extract: characterization and in vitro evaluation of cytotoxicity and antibacterial properties. *Molecules*, *26*(20), 6140.
31. Selim, Y. A., Azb, M. A., Ragab, I., & HM Abd El-Azim, M. (2020). Green synthesis of zinc oxide nanoparticles using aqueous extract of Deverra tortuosa and their cytotoxic activities. *Scientific reports*, *10*(1), 3445.
32. Parajuli, D., Dangi, S., Sharma, B. R., Shah, N. L., & KC, D. (2023). Sol-gel synthesis, characterization of ZnO thin films on different substrates, and bandgap calculation by the Tauc plot method. *Bibechana*, *20*(2), 113-125.
33. Rehman, H., Shah, R. U., Khan, A., Hussain, A., & Ullah, H. (2019). Synthesis and characterization of ZnO nanoparticles and their use as an adsorbent for the arsenic removal from drinking water. *Digest Journal of Nanomaterials and Biostructures, 14*(4), 1033–1040.
34. Geetha, A., & Mallika, J. (2015). Synthesis and characterization of ZnO nanoparticles. *A Journal of Science and Technology, 3*(2), 72–76.
35. Alharthi, F. A., Alghamdi, A. A., Alothman, A. A., Almarhoon, Z. M., Alsulaiman, M. F., & Al-Zaqri, N. (2020). Green synthesis of ZnO nanostructures using *Salvadora persica* leaf extract: Applications for photocatalytic degradation of methylene blue dye. *Crystals, 10*(3), 189. https://doi.org/10.3390/cryst10030189
36. Darvishi, E., Kahrizi, D., & Arkan, E. (2019). Comparison of different zinc oxide nanoparticles synthesized by the green (using *Juglans regia* L. leaf extract) and chemical methods. *Journal of Molecular Liquids, 286*, 110831. https://doi.org/10.1016/j.molliq.2019.04.108
37. Chaudhari, A. A., et al. (2022). Synthesis and characterization of zinc oxide nanoparticles using green synthesis method. *International Journal of Creative Research Thoughts, 10*, 302–309.
38. Yuvakkumar, R., Suresh, J., Saravanakumar, B., Nathanael, A. J., Hong, S. I., & Rajendran, V. (2015). Preparation and characterization of ZnO nanoparticles. *Spectrochimica Acta Part A: Molecular and Biomolecular Spectroscopy, 137*, 250–258. https://doi.org/10.1016/j.saa.2014.08.022
39. Murthy, K. R. S., Raghu, G. K., & Binnal, P. (2021). Zinc oxide nanostructured material for sensor application. *J. Biotechnol. Bioeng*, *5*(1), 25-29. DOI: https://doi.org/10.22259/2637-5362.0501004
40. Agarwal, H., Nakara, A., Menon, S., & Shanmugam, V. (2019). Eco-friendly synthesis of zinc oxide nanoparticles using Cinnamomum Tamala leaf extract and its promising effect towards the antibacterial activity. *Journal of Drug Delivery Science and Technology*, *53*, 101212.
41. Riaz, J., Cao, J., Zhang, Y., Bibi, A., Zhou, X., 2024. Facile synthesis and electrochemical analysis of TiN-based ZnO nanoparticles as promising cathode materials for asymmetric supercapacitors. *Nanoscale Adv.* 6(20), 5145–5157. https://doi.org/10.1039/D4NA00372A

42. Ahmed, S., Alshammari, A. S., Al-Rajhi, A. M. H., et al. (2025). Starch-assisted eco-friendly synthesis of ZnO nanoparticles: Enhanced photocatalytic, supercapacitive, and UV-driven antioxidant properties. *International Journal of Molecular Sciences, 26*(2), 859. https://doi.org/10.3390/ijms26020859
43. Amirtharaj, K., Kumar, M. S., & Prabhu, M. R. (2023). Electrochemical performance of flower-like ZnO nanostructure crystal for supercapacitor electrode applications. *Asian Journal of Chemistry, 35*(8), 1887–1893. https://doi.org/10.14233/ajchem.2023.28050
44. Priyadharshini, S. S., Shubha, J. P., Shivalingappa, J., Adil, S. F., Kuniyil, M., Hatshan, M. R., Shaik, B., & Kavalli, K. (2022). Photocatalytic degradation of methylene blue and metanil yellow dyes using green synthesized zinc oxide (ZnO) nanocrystals. *Crystals, 12*(1), 22. https://doi.org/10.3390/cryst12010022
45. Atta, D., Wahab, H. A., Ibrahim, M. A., & Battisha, I. K. (2024). Photocatalytic degradation of methylene blue dye by ZnO nanoparticle thin films using sol–gel technique and UV laser irradiation. *Scientific Reports, 14*, 26961. https://doi.org/10.1038/s41598-024-76938-1
46. S. S. Shinde, K. Y. Rajpure, X-ray photoelectron spectroscopic study of catalyst based zinc oxide thin films, Journal of Alloys and Compounds, 2011, 509, 4603-4607, doi: 10.1016/j.jallcom.2011.01.117.
47. Rana, M. S., Putul, R. A., Salsabil, N., Kabir, M. T., Hossain, M. S., Masum, S. M., & Molla, M. A. I. (2026). Solar-Driven Photodegradation of Methylene Blue Dye Using Al-Doped ZnO Nanoparticles. *Applied Nano*, *7*(1), 3.
48. Balcha, A., Yadav, O. P., & Dey, T. (2016). Photocatalytic degradation of methylene blue dye by zinc oxide nanoparticles obtained from precipitation and sol-gel methods. *Environmental Science and Pollution Research*, *23*(24), 25485-25493.
49. Abdallah, M., Alqahtani, A. S., Alharbi, S. A., Alghamdi, S., & Al-Hazmi, N. E. (2024). Biosynthesis of zinc oxide nanoparticles using seaweed: Exploring their therapeutic potentials. *Applied Sciences, 14*(16), 7069. https://doi.org/10.3390/app14167069
50. El-Hagrasi, A.M., et al., 2024. Design, synthesis, pharmacological evaluation, and in silico studies of novel spiro pyrrolo[3,4-d]pyrimidine derivatives. *RSC Advances* 14, 2024. https://doi.org/10.1039/D3RA07078F
51. Vieira, I. R. S., da Silva, A. A., da Silva, B. D., Torres Neto, L., Tessaro, L., Lima, A. K. O., ... & Conte-Junior, C. A. (2024). Antioxidant, antimicrobial, and anticancer potential of green synthesized ZnO nanoparticles from Açaí (Euterpe oleracea Mart.) berry seed residue extract. *Waste and Biomass Valorization*, *15*(8), 4717-4734.
52. Sugitha, S. J., Latha, R. G., Venkatesan, R., Kim, S. C., Vetcher, A. A., & Khan, M. R. (2024). Green synthesis of Al-ZnO nanoparticles using Cucumis maderaspatanus plant extracts: analysis of structural, antioxidant, and antibacterial activities. *Nanomaterials*, *14*(22), 1851.
53. Elango, G., Kumar, P.S., Kumar, V., et al., 2024. Phytochemical fabrication of ZnO nanoparticles and their antibacterial and anti-biofilm activity. *Scientific Reports* 14, 19714. https://doi.org/10.1038/s41598-024-69044-9